Computational Modelling of Acoustic Scattering of a Sound Source in the Vicinity of the Ground

Dr. Panagiota Pantazopoulou and Prof. Dimitris Drikakis Members, IAENG *

Abstract—**The paper presents a computational model for acoustic scattering of a near-the-ground sound source around a body moving in a uniform flow. Using the method of images and the concept of reflection coefficient, the half space Green's function in a uniform flow is derived in the framework of the boundary element method (BEM). The method is validated against analytical solutions and is further applied in the case of acoustic scattering around an airfoil moving in the vicinity of the ground both for rigid and soft ground conditions. The results show the importance of ground impedance in the attenuation of sound.**

Keywords: sound, method of images, Boundary Element Methods, uniform flow, aerofoil

1 Introduction

Studies of sound scattering and radiation over infinite planes [1] have been carried out in the past in relation to surfaces of variable [2] and constant [3] impedance. The acoustic source can be either stationary or move above the ground radiating sound waves, which can be reflected, refracted or absorbed depending on the ground topography [4]. Therefore, the impedance factor needs to be taken into account when modeling acoustic fields near and far from the acoustic source.

Another important parameter is the acoustic frequency. In application problems such as traffic noise and aircraft take off, high frequencies are more likely to dominate. When the distance between the infinite plane and the source is quite small then the sound frequency is generally high [5]. Because of this, large computational resources are required to obtain satisfactory acoustic predictions.

Boundary element methods (BEM) have been extensively used in the investigation of half-space scattering problems [6], [7]. Half-space problems in acoustics concern an acoustic source located above an infinite plane which normally represents the ground. The most important feature of BEM in acoustics is that the computational cost is significantly reduced as only the surface of the obstacle causing scattering needs to be modeled. The far field is treated by the Sommerfeld radiation condition [8] that is automatically satisfied. The majority of BEM formulations are based on the classical Helmholtz integral equation and follow a direct [9] or an indirect [10] solution using the Green's function. Seznec [11] employed the method of images to derive the half-space Green's function, which provided satisfactory results when comparing with geometrical approaches. Seybert *et al.* [12] extended the method of images by introducing the reflection coefficient, R_H. The reflection coefficient is valid for a boundary that has homogeneous impedance; it varies from -1 to 1 depending on the rigidity of the plane, where the values -1 and 1 correspond to soft and rigid planes, respectively. For a frequency range of $100Hz$ to $4kHz$, the wall reflection coefficients are greater than 0.7 [13]. This result is based on geometrical acoustic theory [14], where frequency and reflection angle variations are not taken into account.

If the ground plane does not encompass homogeneous impedance, the method of images is no longer sufficient to capture the effects of an absorbing ground because the original Green's function does not include all the necessary terms. This can be rectified by adding a correction term to the Green's function, which consists of an infinite integral with an oscillatory integrand [15]. Research efforts are subsequently focusing on the successful derivation of the half-space Green's function when the infinite plane is not perfectly rigid but it has a variable impedance. The half-space Green's function includes an integral form of the inverse Fourier transform but since the integral cannot be analytically integrated, it can be transformed to a suitable form for effective evaluation [16].

The aforementioned efforts were limited to stationary acoustic sources located above a flat plane or trapped within walls. In this paper a BEM formulation based on the Helmholtz equation for a uniformly moving acoustic source that is also applicable to relatively high frequencies through an improved first-order element discretisation, is presented. The boundary integral equation for prediction of sound in uniform flows based on the Green's function theorem, has been applied to radiation problems of moving sources [17]. The Green's function for the uni-

*Manuscript received June 24, 2009.
Panagiota Pantazopoulou is Senior consultant, BRE, Watford, UK, E-mail: pantazopouloup@bre.co.uk,
Dimitris Drikakis is Professor, Cranfield University, Aerospace Sciences Department, E-mail: d.drikakis@cranfield.ac.uk, MIAENG.

formly moving source is obtained solving the linear wave equation. An extension of this integral method is employed to solve half space problems for moving acoustic sources combining the classical ground acoustics with the boundary element methods. To do so, the concept of the method of images is adopted where the Green's function is not the stationary medium any more but the one that includes the mean flow effects. The method is valid for rigid and soft boundaries as well as for boundaries with homogeneous impedance. The Green's function is derived by the method of images with a constant reflection coefficient. Both modest and high frequencies are considered and validation is presented against analytical solutions. The method is also applied to acoustic scattering of a sound source pertinent to a simplified[1] road traffic and airport runway noise during landing and take off.

2 Numerical Formulation

A body, B, with boundary surface, S in an infinite acoustic medium B' of mean density ρ_0 and speed of sound c, is considered (Figure 1. The body can be either a vibrating structure, e.g. a radiation problem, or a passive obstacle, e.g. a scattering problem.

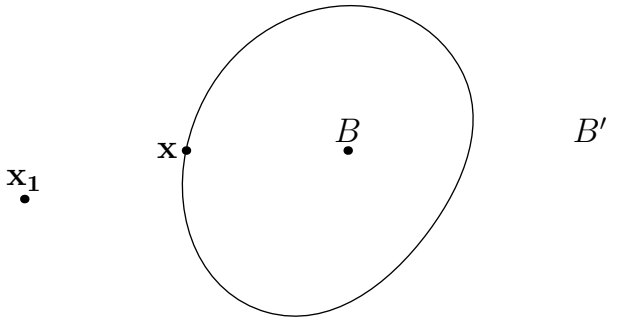

Figure 1: Schematic of a body in an infinite acoustic medium.

Let us now consider the sound radiated into the unbounded fluid from a time-harmonic volume source $q(\mathbf{x}_1, t) = \phi(\mathbf{x}_1, \omega)\exp(-\mathrm{i}\omega t)$ of radian frequency ω. Assuming that the problem is linear, the wave equation for $\phi(\mathbf{x}_1, \omega)$ can be written:

$$\nabla^2\phi - \frac{1}{c^2}\frac{\partial\phi}{\partial t^2} = 0\,, \tag{1}$$

which can be converted to an integral equation in order to introduce a formulation both for compressible and incompressible potential flows [18]. The boundary integral equation (BIE) is the same equation with the one used for acoustic scattering in a uniform flow [19]:

[1]Without including modeling of atmospheric conditions and ground topography.

$$\phi(\mathbf{x}, t) = \int_S \left[\frac{\partial\phi}{\partial\hat{\mathrm{n}}}G - \phi\frac{\partial G}{\partial\hat{\mathrm{n}}} + G\frac{\partial\phi}{\partial t}\left(\frac{\partial\theta}{\partial\hat{\mathrm{n}}} + 2\frac{\mathbf{u}.\mathrm{n}}{c^2}\right)\right]^{\theta} \mathrm{d}S\,, \tag{2}$$

where

$$\frac{\partial}{\partial\hat{\mathrm{n}}} = \frac{\partial}{\partial\mathrm{n}} - \frac{1}{c^2}\mathbf{u}\cdot\mathbf{n}.\mathbf{u}.\nabla, \tag{3}$$

and $[\ldots]^{\theta}$ denotes evaluation at time $\tau = t - \theta$, where θ is the time elapsed for the sound to travel from the source to the observer; $\mathbf{x}$ stands for the position and $\phi(\mathbf{x}, t)$ is the value of the velocity potential at $\mathbf{x}$. The above equation is the boundary integral equation for compressible flows based on the potential formulation.

The Green's function G represents the potential field associated with a uniformly moving acoustic source. For compressible potential flow the Green's function in the positive x direction is given by [8]:

$$G = -\frac{\mathrm{i}}{4}\frac{\mathrm{e}^{\mathrm{i}kM(x-x_1)/\beta^2}}{\beta}\mathbf{H}_0^{(2)}(\frac{kS}{\beta^2})\,, \tag{4}$$

where M is the flow Mach number; $\mathbf{H}_0^{(2)}$ is the Hankel function of second kind; the subscript 1 denotes the source position; and

$$\begin{aligned} S &= \left[(x-x_1)^2 + \beta^2(y-y_1)^2 + z_1^2\right]^{1/2}, \\ R &= \left[(x-x_1)^2 + (y-y_1)^2 + z_1^2\right]^{1/2}, \\ \beta &= \left(1-M^2\right)^{1/2}, \\ \sigma &= \frac{M(x-x_1)+S}{\beta^2}, \\ M &= \frac{u}{c}\,. \end{aligned}$$

In order to simulate the half-space problem without modeling the infinite plane itself, the half-space Green's function is constructed using the method of images (Figure 2).

The distance between P' and any point Q on the surface B is denoted by R'. The half-space Green's function G_H is constructed by adding the image point source solution with a reflection coefficient, R_H, to the original free-space solution:

$$G_H = -\frac{\mathrm{i}}{4}\frac{\mathrm{e}^{\mathrm{i}kM(x-x_1)/\beta^2}}{\beta}\mathbf{H}_0^{(2)}(\frac{kS}{\beta^2}) - R_H\frac{\mathrm{i}}{4}\frac{\mathrm{e}^{\mathrm{i}kM(x-x_1)/\beta^2}}{\beta}\mathbf{H}_0^{(2)}(\frac{kS'}{\beta^2})\,, \tag{5}$$

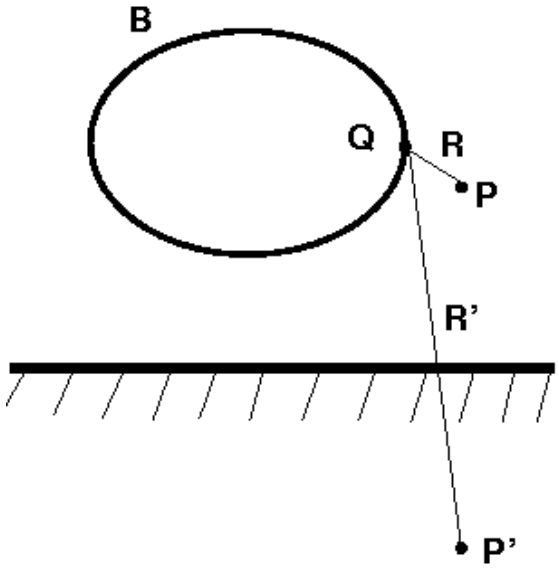

Figure 2: Schematic of the method of images for the half-space Green's function.

where the reflection coefficient, R_H is 1 and -1 for rigid and soft reflection planes, respectively. The reflection coefficient depends on the impedance of the two media, air and ground, and represents the absorbency of the ground in a homogeneous way, i.e. the entire infinite plane is assigned with the same reflection coefficient.

3 Computational studies

Validation of the method was initially obtained against the standard BIE method when modelling the actual half-plane. The problem of a moving acoustic source above a horizontal line is equivalent to that of an acoustic source radiation using the half-space Green's function. Therefore, the pressure field obtained by using the half-space Green's function should be identical with the total, incident plus scattered field, obtained by applying the BIE method. In the standard formulation the horizontal line is discretized and a typical sound radiation problem is solved. The comparisons were performed for frequencies ($ka = 8$,$ka = 16$) and Mach numbers, $M = 0.1$ and $M = 0.3$. Figure 3 shows comparison of the two techniques in terms of contour plots of the acoustic pressure. Very good agreement is obtained including the frequency $ka = 8$ and Mach numbers $M = 0.1$ and $M = 0.3$.

Furthermore, validation was performed against analytical solution for a semi-cylindrical barrier situated in an infinite rigid plane (Figure 4)that is subject to an incident plane wave, $\phi_I = e^{ikx}$.

The analytic solution for the sound field, ϕ, due to the wave $\phi_I = e^{ikx}$ over a cylinder of a finite constant admittance β_1 is given by [5]

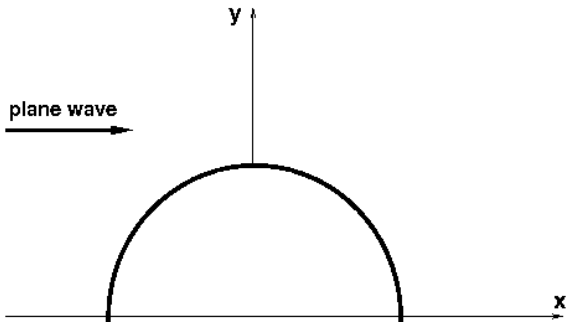

Figure 4: Schematic of the problem of a plane wave over a semi-cylinder barrier situated in an infinite plane.

$$\phi = \sum_{m=0}^{\infty} A_m \cos(m\theta) \mathrm{H}_0^1(kr) + \phi_I \ , \tag{6}$$

where

$$A_0 = -\frac{-\mathrm{J}_1(ka) + \mathrm{i}\beta_1 \mathrm{J}_0(ka)}{-\mathrm{H}_1^1(ka) + \mathrm{i}\beta_1 \mathrm{H}_0^1(ka)} \ , \tag{7}$$

and

$$A_m = -2_i^m \frac{-\mathrm{J}_{m-1}(ka) - \mathrm{J}_{m+1}(ka) + 2\mathrm{i}\beta_1 \mathrm{J}_m(ka)}{-\mathrm{H}_{m-1}^1(ka) - \mathrm{H}_{m+1}^1(ka) + 2\mathrm{i}\beta_1 \mathrm{H}_m^1(ka)} \ , \tag{8}$$

where $x = r\cos\theta$ and $y = r\sin\theta$ in polar co-ordinates, $\mathrm{H}_m^1(ka)$ is the Hankel function of the first kind of order m, the real part term of which is the Bessel function $\mathrm{J}_m(ka)$. Comparisons of the computed and analytical solutions are presented in Figure 6: the maximum error in the numerical solution is $\epsilon = 8\%$ defined by the expression

$$\epsilon = \frac{\phi - \phi_{com}}{\phi} 100\% \tag{9}$$

where ϕ is given by Equation 6 and ϕ_{com} is the sound pressure computed using the boundary integral method. The numerical error depends on the number of line elements used in the boundary. Figure 5 shows the behaviour of the maximum error with the number of discretization elements when $ka = 10$.

As it can be seen from Figure 5 the maximum error drops significantly as the boundary discretization gets finer. It is important to note though that the results presented below were produced using a grid of 900 elements to eliminate any numerical errors.

Furthermore, the above method has been implemented to investigate acoustic scattering of a sound source around a supercritical airfoil[2] placed in uniform flow and in the vicinity of the ground (Figure 7). The airfoil was discretized using $1,200$ elements.

[2]The airfoil geometry was available through the European Fifth Framework Programme, ROSAS.

$ka = 8$

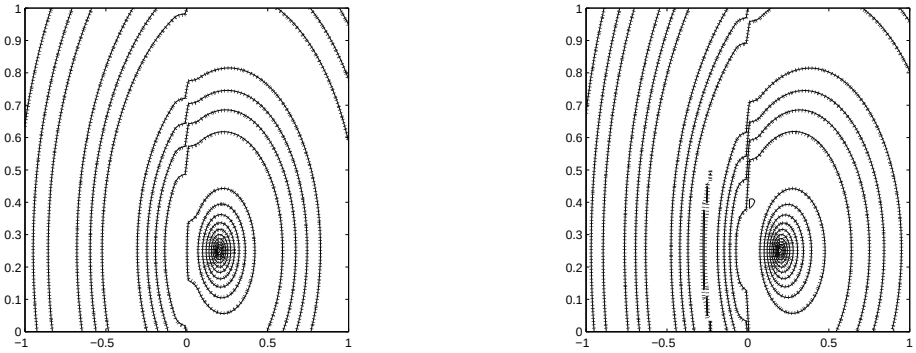

$M = 0.1$ $M = 0.3$

Figure 3: Comparison between analytical and computed acoustic pressure results over a rigid horizontal plane. Solid and dashed line indicate analytical and computed values respectively.

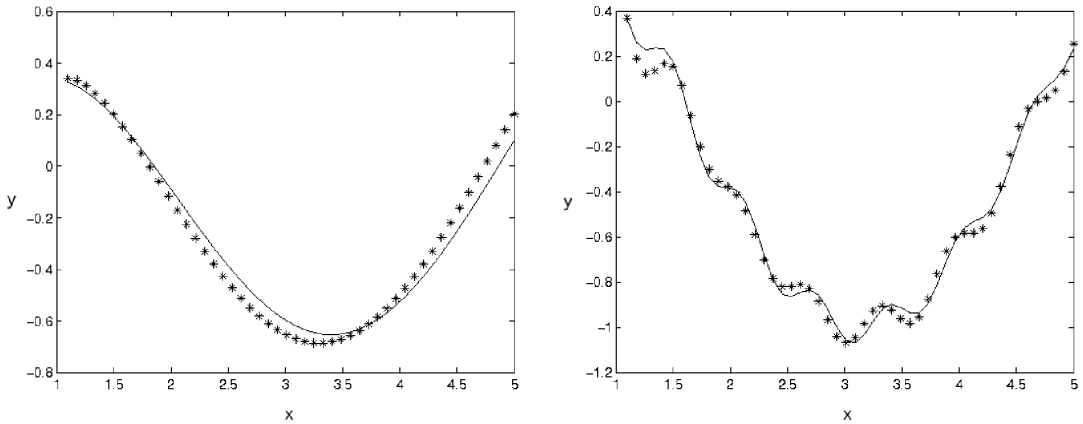

$ka = 1$ $ka = 10$

Figure 6: Comparison of analytical (stars) and computational (solid line) solutions for the acoustic pressure over a semi-cylindrical barrier subjected to an acoustic plane wave.

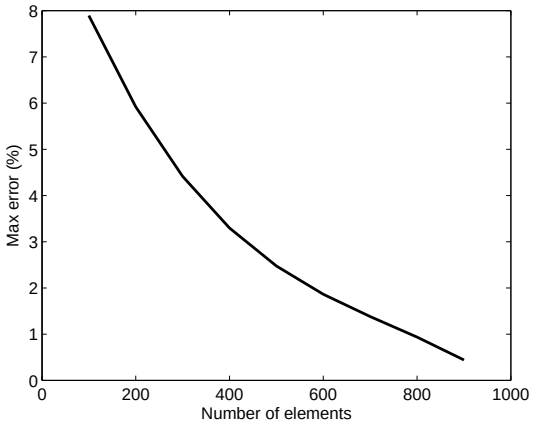

Figure 5: Maximum error in acoustic pressure from a plane wave on a semi-cylinder for different numbers of boundary elements, $ka = 10$.

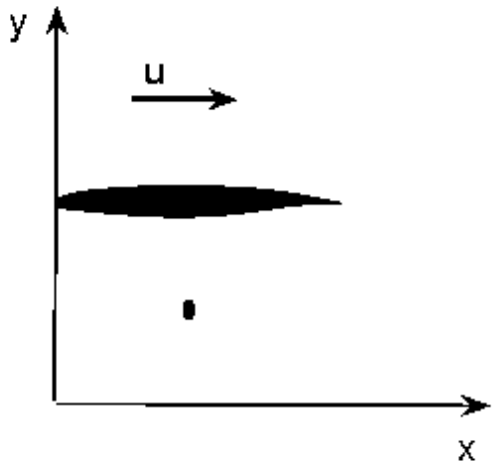

Figure 7: Airfoil and sound source in uniform flow over an infinite plane.

This is an (over) simplified model of an aircraft on the runway shortly before take off, where the engines operating at high frequencies result in high noise levels. The investigation has been carried out for Mach number $M = 0.25$, frequencies $f = 8.8kHz$ and $f = 4kHz$ thereby mimicking realistic take off conditions [20], and reflection coefficients $R_H = 1$ and $R_H = 0.3$

Figure 9 and Figure 8 show polar plots of the acoustic pressure in the near and far fields. As the observer moves away from the source, the sound pressure is significantly attenuated between near and far fields; The higher the frequency, the wider and greater, in magnitude, the acoustic field (see $ka = 30$ vis-à-vis $ka = 65$).

The qualitative similarities between $R_H = 1$ and $R_H = 0.3$ (Figures 9,8 and 10) are due to the linearised wave equation solved. The sound level is, however, significantly lower for $R_H = 0.3$. The lobe (the rounded area which spreads out) formed in the acoustic field for small angles ($< 40°$) is due to the positioning of the acoustic source underneath the airfoil at 50°. There is a shielding effect due to the presence of the airfoil, which causes the acoustic field to be trapped between the airfoil boundary and the ground. The airfoil acts as a protective layer forcing the sound to radiate in directions where there is no obstacle.

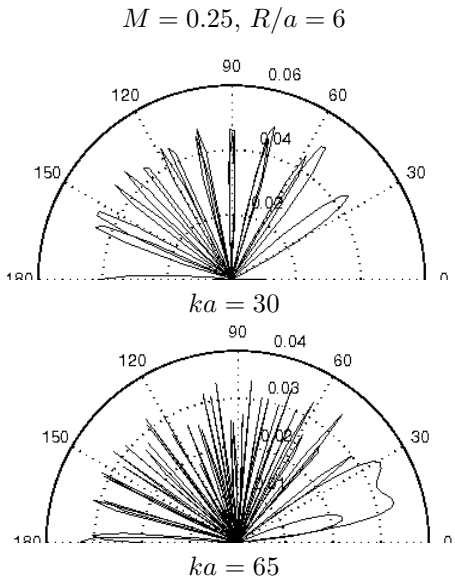

Figure 8: Polar plots of the acoustic pressure over a rigid horizontal plane with an airfoil and an acoustic source in a uniform motion.

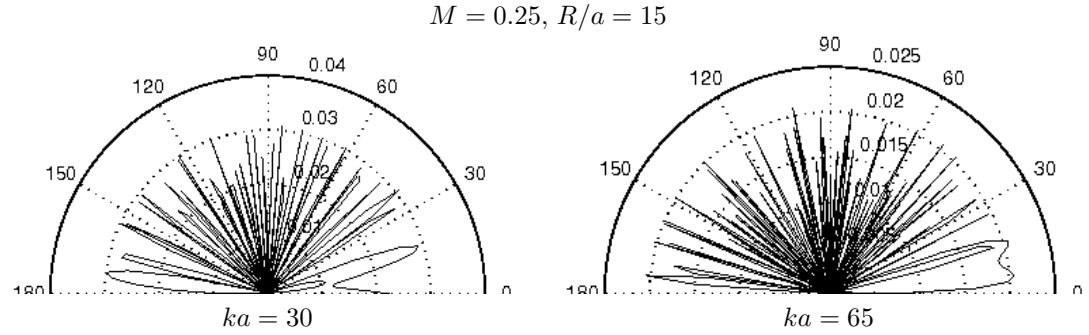

Figure 9: Polar plots of the acoustic pressure over a rigid horizontal plane with an airfoil and an acoustic source in a uniform motion.

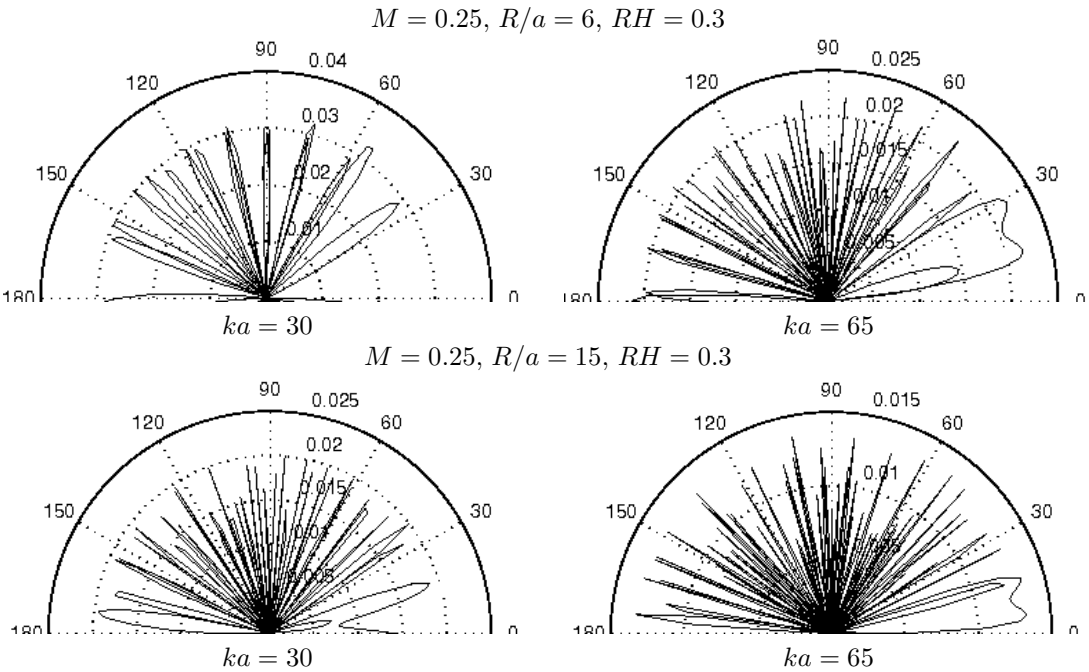

Figure 10: Polar plots of the acoustic pressure over a non-rigid horizontal plane with an airfoil and an acoustic source in a uniform motion.

To further investigate the effects of ground, mean flow and reflections from the boundaries of the airfoil, we have set two rows of 'microphones' at a distance of a chord length below ($y = 0.1$m) and above ($y = 0.9$m) the airfoil chord line. Figure 11 shows in detail the coordinate system, the source position and the microphone series with respect to the airfoil location. Four computational cases were performed using the above 'microphone' set-up: with and without uniform flow as well as with and without the ground effect.

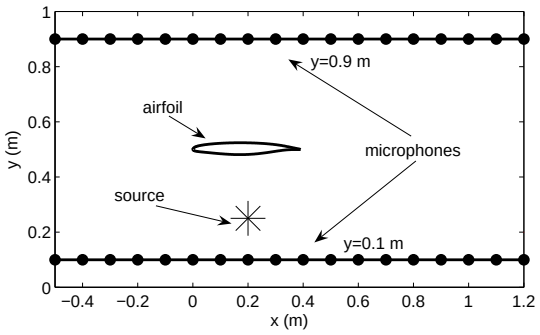

Figure 11: Airfoil 'microphone' locations over an infinite plane.

The acoustic pressure is higher when mean flow is included (Figures 12 and 13). The uniform flow intensifies the acoustic field, especially downstream of the airfoil, by stretching the sound waves and distributing the scattered sound backwards compared to the case without uniform flow (Figure 12). The reflections from the boundaries of the airfoil also contribute to higher acoustic pressures downstream.

The results show (Figures 12 and 13, $y = 0.9$m) that higher pressures occur when the ground (infinite plane) is present. The ground effect contributes to up to 20% (upper row of 'microphones') increase of the maximum pressure level.

4 Conclusions

A uniform-flow boundary integral method has been developed for predicting acoustic field scattering of a sound source around an airfoil placed over an infinite plane. The model accounts both for rigid and for soft ground conditions. The importance of the ground impedance on the attenuation of sound was shown by considering a soft ground condition. This prompts to the use of absorbent materials on runways and roads in order to reduce noise levels. The uniform flow in conjunction with the ground effect intensify the acoustic field downstream of the sound source. The ground effect increases the sound level with-

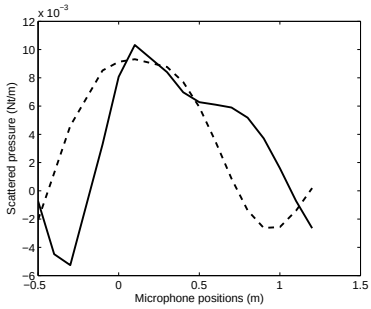

$y = 0.1m$

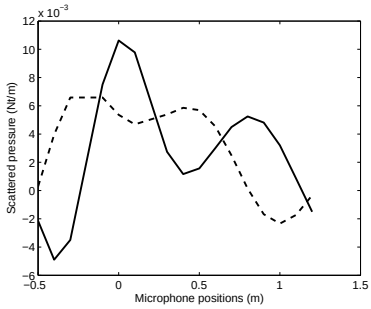

$y = 0.9m$

Figure 12: Scattered pressure over an infinite plane with an acoustic source of frequency, $ka = 8$ and an airfoil; solid and dashed lines correspond to $M = 0.25$ and $M = 0.0$ flow conditions, respectively.

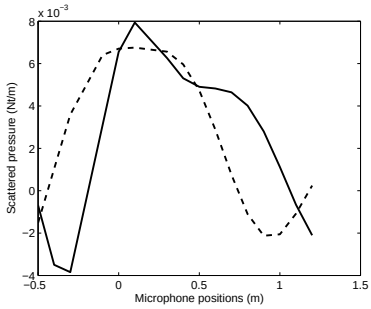

$y = 0.1m$

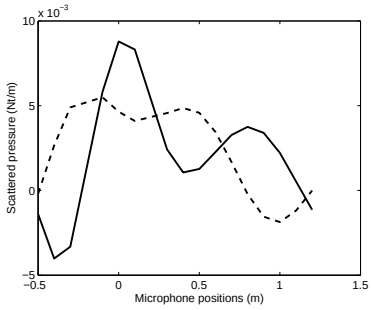

$y = 0.9m$

Figure 13: Scattered pressure around an aerofoil with an acoustic source of frequency, $ka = 8$; solid and dashed lines denote $M = 0.25$ and $M = 0.0$ flow conditions, respectively.

out altering the sound patterns, while the more rigid the ground the higher the acoustic pressure.

At present, the model does not take into account topography characteristics. However, it has the potential to be extended by including the inhomogeneous impedance effects into the Green's function.

References

[1] Ingard, U., "On the reflection of a spherical sound wave from an infinite plane," *Journal of the Acoustical Society of America*, Vol. 23, No. 3, 1951, pp. 329–335.

[2] Hothersall, D. C. and Harriott, J. N. B., "Approximate models for sound propagation above multi-impedance plane boundaries," *Journal of the Acoustical Society of America*, Vol. 97, No. 2, 1994, pp. 918–926.

[3] Habault, D. and Filippi, P. J. T., "Ground effect analysis: surface wave and layer potential representations," *Journal of Sound and Vibration*, Vol. 79, No. 4, 1981, pp. 529–550.

[4] Attenborough, K., "Sound Propagation Close to the Ground," *Annual Review of Fluid Mechanics*, Vol. 34, 2002, pp. 51–82.

[5] Park, J. M. and Eversman, W., "A boundary element method for propagation over absorbing boundaries," *Journal of Sound and Vibration*, Vol. 175, No. 2, 1994, pp. 197–218.

[6] von Estorff, O., Coyette, J. P., and Migeot, J. L., *Boundary elements in acoustics*, chap. 1, 2002.

[7] Wu, T. W., *Boundary Elements in Acoustics: Fundamentals and Computer Codes*, chap. 3, WIT, Southampton, 2000, pp. 29–48.

[8] Howe, M. S., *Acoustics of Fluid-Structure Interactions*, Cambridge University Press, 2nd ed., 1998.

[9] Li, W. L., Wu, T. W., and Seybert, A. F., "A half-space boundary element method for acoustic problems with a reflecting plane of arbitrary impedance," *Journal of Sound and Vibration*, Vol. 171, No. 3, 1994, pp. 173–184.

[10] Granat, C., Tahar, M. B., and Ha-Duong, T., "Variational formulation using integral equations to solve sound scattering above an absorbing plane," *Journal of the Acoustical Society of America*, Vol. 105, No. 5, 1999, pp. 2557–2564.

[11] Seznec, R., "Diffraction of sound around barriers: use of thr boundary elements technique," *Journal of Sound and Vibration*, Vol. 73, 1980, pp. 195–209.

[12] Seybert, A. F. and Wu, T. W., "Modified Helmholtz integral equation for bodies sitting on an infinite plane," *Journal of the Acoustical Society of America*, Vol. 85, No. 1, 1988, pp. 19–23.

[13] Allen, J. B. and Berkley, D. A., "Image method for efficiently simulating small-room acoustics," *Journal of the Acoustical Society of America*, Vol. 65, 1978, pp. 943–950.

[14] Morse, P. M. and Ingard, K. U., *Theoretical Acoustics*, McGraw-Hill, New York, 1968.

[15] Lacerda, L. A. D., "A dual boundary element formulation for sound propagation around barriers over an impedance plane," *Journal of Sound and Vibration*, Vol. 202, No. 2, 1997, pp. 235–247.

[16] Lacerda, L. A., Wrobel, L. C., Power, H., and Mansur, W. J., "A novel boundary integral formulation for three-dimensional analysis of thin acoustic barrieres over an impedance plane," *Journal of the Acoustical Society of America*, Vol. 104, No. 2, 1998, pp. 671–678.

[17] Wu, T. W. and Lee, L., "A direct boundary integral formulation for acoustic radiation in subsonic uniform flow," *Journal of Sound and Vibration*, Vol. 175, No. 1, August 1994, pp. 51–63.

[18] Morino, L., "Boundary integral equations in aerodynamics," *Applied Mechanics Reviews*, Vol. 46, No. 8, 1993, pp. 445–466.

[19] Garrick, I. E. and Watkins, C. E., "A theoretical study of the effect of forward speed on the free-space sound pressure field around propellers," Tech. rep., NACA, 1953.

[20] Delfs, J. and Heller, H., "Aeroacoustics research in Europe-1996 highlights," *Aerospace Science and Technology*, Vol. 2, No. 2, February 1998, pp. 145–154.